Original Article

Hepatosplenic Volumes and Portal Pressure Gradient Identify One-year Further Decompensation Risk Post-transjugular Intrahepatic Portosystemic Shunt

Xinyu Chen[1#], Yicheng Lin[1#], Kefeng Jia[2#], Rong Lv[2], Jiajun Tian[2], Fenghui Li[2], Jun Li[1], Yiwen Zhang[1], Ning Wang[2], Zhongsong Gao[2], Weili Yin[2], Fang Wang[2], Ping Zhu[2], Chao Yang[2], Jiayin Wang[2], Tao Wang[2], Junqing Yan[2], Ying Liu[2], Qing Ye[2] and Huiling Xiang[2*]

[1]*The Third Central Clinical College of Tianjin Medical University, Tianjin University Central Hospital (Tianjin Third Central Hospital), Tianjin Key Laboratory of Extracorporeal Life Support for Critical Diseases, Institute of Hepatobiliary Disease, Tianjin, China;* [2]*Department of Gastroenterology and Hepatology, Tianjin University Central Hospital (Tianjin Third Central Hospital), Tianjin Key Laboratory of Extracorporeal Life Support for Critical Diseases, Institute of Hepatobiliary Disease, Tianjin, China*

Abstract

Background and Aims: Further decompensation in cirrhosis is associated with increased mortality. However, reliable tools to predict further decompensation after transjugular intrahepatic portosystemic shunt (TIPS) are currently limited. This study aimed to investigate the incidence and risk factors of further decompensation within one year post-TIPS in patients with cirrhosis and to develop a predictive model for identifying high-risk individuals. ***Methods:*** This retrospective cohort study enrolled 152 patients with cirrhosis undergoing TIPS for variceal bleeding and/or refractory ascites (January 2018–January 2024). Patients were stratified according to one-year decompensation outcomes. LASSO regression and multivariable logistic analysis were used to identify predictors, and a nomogram was constructed and internally validated using bootstrapping (1,000 replicates). ***Results:*** Among the 152 patients (median age 57.5 years [IQR 50.0–66.0]; 58.6% male; 58.6% viral/alcohol-associated etiology), 65.8% (100/152) achieved clinical stability at one year post-TIPS, while 34.2% (52/152) developed further decompensation. LASSO regression identified right hepatic lobe volume, spleen volume, and portal pressure gradient (PPG) reduction as key predictors, all independently associated with further decompensation risk in multivariable analysis (OR [95% CI]: 0.683 [0.535–0.873], 1.435 [1.240–1.661], and 0.961 [0.927–0.996], respectively). The nomogram demonstrated superior discrimination compared with PPG reduction alone and benchmark prognostic scores (AUC 0.854 [0.792–0.915] vs. 0.619–0.652; ΔAUC +0.201−+0.235, $p < 0.001$) with 92.3% sensitivity. High-risk patients (score > 86) had a 10.7-fold higher risk of further decompensation than low-risk patients (60.0% vs. 5.6%; $p < 0.0001$). ***Conclusions:*** This validated model, combining hepatosplenic volumetry and PPG reduction, accurately stratifies further decompensation risk post-TIPS and may guide targeted surveillance and preventive interventions.

Introduction

Portal hypertension is a critical pathophysiological determinant in cirrhosis progression, with its severity directly correlating with decompensation risk.[1] A hepatic venous pressure gradient (HVPG) > 10 mmHg defines clinically significant portal hypertension, while an HVPG > 12 mmHg markedly increases the risk of variceal hemorrhage and ascites development.[2] Transjugular intrahepatic portosystemic shunt (TIPS) serves as a cornerstone intervention for portal pressure (PP) modulation.[3,4] However, persistent portal hypertension after TIPS occurs in a subset of patients, predisposing them to Baveno VII-defined further decompensation endpoints, including refractory ascites, recurrent variceal hemorrhage, and overt hepatic encephalopathy (HE).[2,5] Current prognostic models predominantly focus on serological biomarkers, such as age, total bilirubin, and albumin levels, to predict post-TIPS further decompensation and hepatic failure.[6,7] Imaging-derived morphometric parameters, however, remain underutilized. The pathophysiological progression of cirrhosis is characterized by dynamic volumetric changes, where hepatic atrophy parallels splenic enlargement, reflecting the severity of parenchymal fibrosis and portal hypertension.[8–10] Emerging evidence positions hepatic and splenic volumetry

as reliable noninvasive indices for: (i) detecting clinically significant portal hypertension (clinically significant portal hypertension, HVPG ≥10 mmHg) with diagnostic accuracy up to AUC 0.89[11,12]; (ii) stratifying decompensation risk in compensated cirrhosis[11]; and (iii) predicting overt HE development post-TIPS.[3] Nevertheless, the prognostic utility of these quantitative imaging biomarkers for identifying post-TIPS further decompensation in already decompensated cirrhosis remains undefined. This study systematically evaluates the incidence of one-year post-TIPS further decompensation and establishes a predictive framework integrating hemodynamic and morphometric parameters to enable early identification of high-risk patients, thereby optimizing candidate selection and personalizing surveillance protocols.

Methods

Study design

This single-center, retrospective cohort study (conducted in accordance with the STROBE guidelines) enrolled consecutive patients with cirrhosis undergoing TIPS at Tianjin Third Central Hospital (January 2018–January 2024) for portal hypertension-related decompensation (variceal bleeding and/or refractory ascites).

The baseline was defined as the time of TIPS placement. The primary endpoint was further hepatic decompensation within one year post-TIPS. Follow-up was terminated at the earliest of:

1. Occurrence of further decompensation (primary endpoint);
2. Death or liver transplantation;
3. Completion of one year of follow-up without decompensation.

Grouping criteria: According to the definition of Baveno VII,[2] further decompensation was defined by meeting one of the following two criteria: 1) Occurrence of a second portal hypertension-driven decompensation event (ascites, variceal bleeding, or HE [stratified as early HE (≤90 days post-TIPS, TIPS procedure-related) or late HE (>90 days, disease progression-related)])[13]; and 2) Recurrent variceal bleeding, worsening of ascites (≥three high-volume punctures required within one year), recurrent HE (similarly stratified),[13] and development of spontaneous bacterial peritonitis (SBP) and/or hepatorenal syndrome-acute kidney injury (HRS-AKI). All events required clinical manifestations and imaging exclusion of TIPS thrombosis; asymptomatic stent abnormalities were not considered decompensation events. We classified all patients into two groups: (1) The further decompensation group: Patients meeting Baveno VII criteria for further decompensation within one year post-TIPS. (2) The clinically stable group: Patients who did not meet these criteria, with confirmation of survival through the one-year follow-up period.

In the mechanistic subanalysis, patients with further decompensation were stratified by the type of the first further decompensation event: portal hypertensive events (PHE: new-onset or worsening ascites, variceal hemorrhage, SBP)[2,14] or HE. HRS-AKI was defined as functional renal impairment without structural disease, typically manifesting as a secondary decompensation.[15] Therefore, HRS-AKI did not occur as the first decompensation event.

Eligibility criteria

Inclusion criteria (all required): (1) Age: 18–80 years old; (2) Confirmed diagnosis of cirrhosis per the Guidelines for the Diagnosis and Treatment of Cirrhosis of the Liver (2020)[16] based on clinical presentation, laboratory tests, imaging examinations (e.g., ultrasonography, computed tomography (CT), or magnetic resonance imaging), endoscopic, and/or biopsy findings; (3) Undergoing elective TIPS placement for decompensated cirrhosis with variceal bleeding and/or refractory ascites.

Exclusion criteria (any met): (1) Absence of triphasic abdominal CT within three months preceding TIPS; (2) Prior splenectomy; (3) Pre-existing hepatocellular carcinoma diagnosed before TIPS placement; (4) Incomplete follow-up data; (5) Unavailability of liver volume or clinical data. (6) Presence of non-cirrhotic portal hypertension (e.g., extrahepatic portal vein obstruction, congenital hepatic fibrosis).

Observation indicators, concepts, and therapies

Observational indicators: Demographics (gender, age); Past history (smoking, alcohol use, diabetes mellitus, coronary heart disease, hypertension); Laboratory parameters: complete blood count, hepatic and renal function, prothrombin time activity, serum sodium, blood ammonia; Hemodynamic indices: PP, inferior vena cava pressure (IVCP), PPG, PPG reduction; Imaging indices: spontaneous portosystemic shunt, portal vein thrombosis, portal vein cavernous transformation.

Etiology-specific therapeutic interventions: (a) Etiology-eliminating therapy: Administration of antiviral agents for ≥three months pre-TIPS in patients with hepatitis B virus (HBV) or hepatitis C virus (HCV) infection, or sustained abstinence ≥ three months pre-TIPS (verified by medical records and structured telephone follow-up) in alcohol-associated liver disease; (b) Disease-controlling therapy: Receiving guideline-directed[17] immunosuppression or ursodeoxycholic acid (UDCA) for ≥three months for autoimmune hepatitis or primary biliary cholangitis.

Assessment models: Child-Pugh score[18]; model for end-stage liver disease (MELD) = 9.57×ln (creatinine[mg/dL]) + 3.78×ln(bilirubin[mg/dL]) + 11.2×ln(international normalized ratio (INR)) + 6.431[19]; MELD-Na = MELD + 1.32× (137-Na[mmol/L]) - [0.033 × MELD × (137-Na[mmol/L])].[5] MELD 3.0 = 1.33 (if female) + 4.56 × $\log_e$(bilirubin) + 0.82 × (137 − Na) − 0.24 × (137 − Na) × $\log_e$(bilirubin) + 9.09 × $\log_e$(INR) + 11.14 × $\log_e$(creatinine) + 1.85 × (3.5 − albumin) − 1.83 × (3.5 − albumin) × $\log_e$(creatinine) + 6.[20]

TIPS procedural protocol

The TIPS procedure was performed under local anesthesia via right internal jugular vein access. Under fluoroscopic guidance, a guidewire and sheath were sequentially advanced into the hepatic veins, followed by transhepatic puncture into a portal venous branch. Portal venography and real-time pressure measurements (PP, IVCP) were obtained using calibrated transducers, with the PPG calculated as PPG = PP - IVCP. The parenchymal tract was subsequently dilated using 8mm/6mm balloon catheters (Lepu Medical, China) and stented with either Fluency Plus covered stents of 8mm diameter (Bard, USA) or Viatorr endoprostheses (Gore & Associates, USA). Post-deployment PPG was remeasured to calculate the hemodynamic response: PPG reduction = [(Pre-shunt PPG - Post-shunt PPG)/Pre-shunt PPG]×100.

Abdominal enhanced CT examination and measurement of liver and spleen volumes

All patients underwent imaging using the Siemens Healthcare Definition Flash dual-source CT scanner, covering the area from the top of the diaphragm to the lower edge of the liver and spleen. The scanning parameters included a slice thickness of 5.0 mm, slice spacing of 5.0 mm, pitch of 1.375:1, voltage of 120 kVp, and current of 250 mAs.
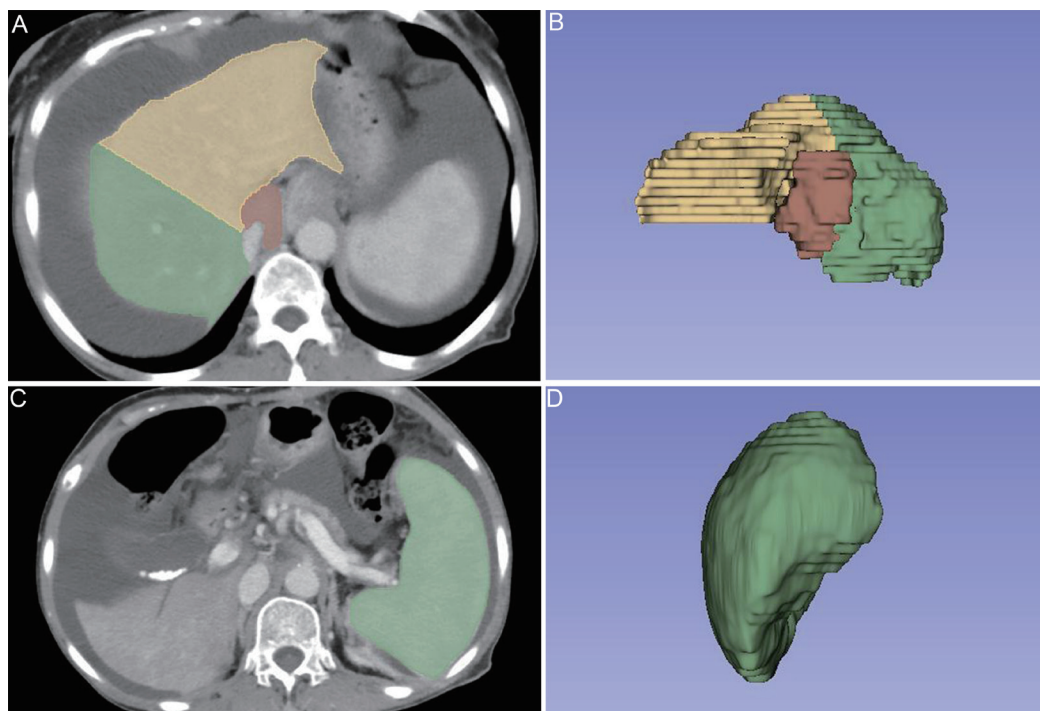
Fig. 1. Hepatic and splenic segmentation using 3D Slicer software. (A) Axial view demonstrating hepatic segmentation results: green, right hepatic lobe; yellow, left hepatic lobe; brown, caudate lobe. (B) Three-dimensional hepatic segmentation. (C) Axial view of splenic segmentation (green). (D) Three-dimensional splenic segmentation.

A total of 90 mL of iodine contrast agent was administered via the antecubital vein at a rate of 2.5–3.0 mL/s. Dynamic scanning was conducted in three phases: arterial (25–30 s), portal venous (70–75 s), and delayed (3 m). Subsequently, thin-layer reconstruction was performed with a reconstructed slice thickness and spacing of 1.25 mm, along with parallel coronal and sagittal image reconstructions.

Hepatic lobar segmentation adhered to the Couinaud classification,[21] defining the right hepatic lobe as segments V, VI, VII, and VIII, and the left hepatic lobe as segments II, III, and IV, demarcated by the principal plane (Cantlie line) along the middle hepatic vein trajectory from the gallbladder fossa to the inferior vena cava. The caudate lobe (segment I) was defined by its anatomical boundaries: posteriorly by the inferior vena cava fossa, anteriorly by the hepatic hilum, and inferiorly by the left portal vein (Fig. 1).

Volumetric quantification utilized portal venous phase contrast-enhanced CT images (5-mm slice thickness, helical acquisition) processed through 3D Slicer software (v5.3.0). Semi-automated segmentation with manual refinement was performed on axial slices to delineate hepatic lobes and splenic parenchyma. Liver and spleen volumes were outlined by a medical student trained by the Chief of Radiology (>10 years of abdominal imaging experience). All segmentations underwent expert verification by the same Chief Radiologist. Volumetric analysis was conducted using voxel-based computation with a spatial resolution of 0.69 mm (in-plane) × 5 mm (slice thickness). Volumes were standardized to 100 cm^3 increments for clinical interpretability. Volumetric stability was assessed by comparing repeat CT scans from 10 patients within three months pre-TIPS.

Statistical analysis

Data analysis utilized R 4.4.2, SPSS 27.0, and GraphPad Prism 10. Continuous variables were expressed as mean ± SD or median (IQR), and categorical variables as n (%). Between-group comparisons employed Student's t-test/Mann-Whitney U test (continuous) and Chi-square/Fisher's exact test (categorical). Predictor selection involved univariable logistic regression with LASSO regularization, followed by multivariable logistic regression to derive adjusted ORs (95% CI). Post hoc power analysis was performed using G*Power (v3.1.9.2) with final model effect estimates under the following parameters: α = 0.05 (two-tailed), n = 152, and normally distributed predictors using cohort-derived means and SDs. Although right hepatic lobe volume and spleen volume were anticipated to exhibit skewness, the large sample size ensured robustness of parametric power estimates against deviations from normality. The resultant model was visualized as a nomogram using RStudio, with internal validation via 1000 bootstrap resamples. Model performance was assessed by ROC-AUC (Youden index-determined cutoff), Kaplan-Meier curves (cumulative incidence), Hosmer-Lemeshow test with calibration plots, and decision curve analysis. Sensitivity analyses addressed TIPS procedure-related confounding by excluding early HE (≤90 days) cases, supplemented by interaction testing and DeLong's test for AUC comparison. Subgroup analyses were stratified by etiology and first decompensation event type, with additional stratification for etiology-specific therapeutic interventions in elimination-amenable etiologies (HBV/HCV, alcohol-associated cirrhosis). All etiology-stratified outcomes were reported descriptively without statistical comparisons due to anticipated small subgroup samples. Intra-observer consistency was assessed using intraclass correlation coefficient (ICC) (2,1). Biological stability was evaluated via Bland-Altman mean difference (bias) and paired tests. Statistical significance was defined as two-tailed $p < 0.05$.
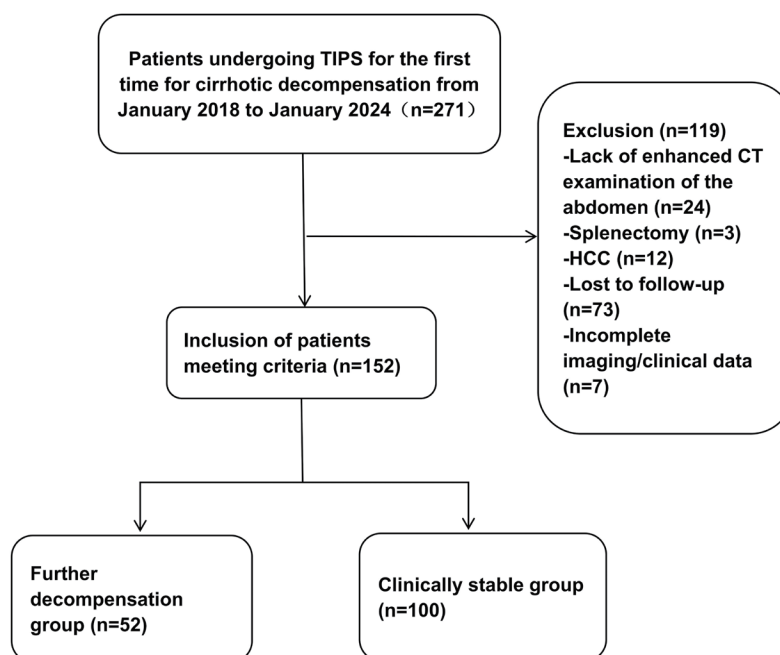
Fig. 2. Process for the selection of patients. CT, computed tomography; TIPS, transjugular intrahepatic portosystemic shunt; HCC, hepatocellular carcinoma.

Model implementation

A web-based risk calculator was developed using R Shiny (version 4.4.2) to operationalize the final prediction model, hosted on the Shinyapps.io platform.

Missing data handling

Missing data were imputed using multiple imputation via the fully conditional specification algorithm in SPSS 27.0. Five imputed datasets were generated, incorporating all baseline predictors and outcome variables (decompensation status). Pooled estimates were calculated using Rubin's rules, with convergence confirmed by trace plots over 10 iterations (Supplementary Table 1).

Results

Patient flow and decompensation event distribution

Among 271 consecutive patients with decompensated cirrhosis undergoing TIPS at Tianjin Third Central Hospital (2018–2024), 152 met the inclusion criteria after exclusions: no pre-TIPS contrast-enhanced CT within three months (n = 24), prior splenectomy (n = 3), hepatocellular carcinoma (n = 12), loss to follow-up (n = 73), and incomplete data (n = 7) (Fig. 2). At one year post-TIPS, 100 patients (65.8%) remained clinically stable, while 52 (34.2%) developed further decompensation. All further decompensation events included new-onset/worsening ascites (24.3%, n = 37), overt HE (10.5%, n = 16), variceal hemorrhage (7.2%, n = 11), SBP (4.6%, n = 7), and HRS-AKI (1.3%, n = 2). Analysis of first decompensation events in these 52 patients identified 38 PHEs (73.1%: new-onset or worsening ascites n = 28, variceal hemorrhage n = 10; no SBP as first presentation) and 14 HE cases (26.9%), with five (35.7%) occurring as early HE (≤90 days post-TIPS) and nine (64.3%) as late HE (>90 days). No decompensation event was attributable to TIPS thrombosis. A single case of asymptomatic stent graft intimal hyperplasia was radiologically detected at two months post-TIPS, but did not progress to clinical significance or require intervention.

Baseline demographic and laboratory characteristics

The study cohort included 152 patients with a median age of 57.50 years (IQR 50.00–66.00), including 89 males (58.55%). The median follow-up was 12.0 months (IQR: 7.8–12.0 months). Etiologies of cirrhosis were distributed as follows: HBV-related cirrhosis (28.94%, n = 44), HCV-related cirrhosis (5.92%, n = 9), alcohol-associated cirrhosis (23.68%, n = 36), autoimmune hepatitis/primary biliary cholangitis-related cirrhosis (20.39%, n = 31), and other causes (21.05%, n = 32). Patients were stratified into clinically stable (65.8%, n = 100) and further decompensation (34.2%, n = 52) groups. Significant intergroup differences (all $p < 0.05$) were observed in the Child-Pugh grade (χ^2 test, $\chi^2 = 7.78$), MELD score (Mann-Whitney U test, $Z = -3.05$), MELD-Na score (Student's t-test, $t = -3.17$), platelet count ($Z = -4.58$), total bilirubin ($Z = -2.61$), and prothrombin time activity ($Z = 2.75$), with no other parameters showing statistical significance (Table 1).

Baseline imaging/hemodynamic characteristics and measurement reliability

Repeat CTs (n = 10, median 2.2-month interval) showed excellent measurement reliability (ICC > 0.95) and volume stability (hepatic LoA: $-1.4 \sim 1.6 \times 100$ cm^3; splenic LoA: $-1.0 \sim 2.6 \times 100$ cm^3; all $p > 0.77$) (Supplementary Table 2). Building on this stable metric, comparative analysis in the full cohort (n = 152) revealed that the further decompensation group showed significantly lower right hepatic lobe volume (Mann-Whitney U test, $Z = -3.50$) and PPG reduction (Student's t-test, $t = 2.91$) while exhibiting higher spleen volume ($Z = -6.04$), post-shunt PP ($t = -3.12$), pre-shunt PPG ($t = -2.11$), and post-shunt PPG ($t = -3.62$) (all $p <$ 0.05, Table 2).

Table 1. Comparison of general information and laboratory testing between the further decompensation group and the clinically stable group

Variables	Total (n = 152)	Clinically stable group (n = 100)	Further decompensation group (n = 52)	Statistic	p
Age/[years, M (Q_1, Q_3)]	57.50 (50.00, 66.00)	59.00 (51.75, 67.00)	56.00 (49.00, 63.25)	Z = −1.41	0.158
Sex/n(%)				X^2 = 0.04	0.848
Male	89 (58.55)	58 (58.00)	31 (59.62)		
Female	63 (41.45)	42 (42.00)	21 (40.38)		
Etiology/n(%)				X^2 = 3.22	0.359
Hepatitis B virus	44 (28.94)	26 (17.11)	18 (11.84)		
Hepatitis C virus	9 (5.92)	7 (4.61)	2 (1.32)		
Alcohol-associated	36 (23.68)	26 (26.00)	10 (19.23)		
AIH/PBC	31 (20.39)	23 (23.00)	8 (15.38)		
Other[a]	32 (21.05)	18 (18.00)	14 (26.92)		
TIPS indication				X^2 = 2.97	0.226
Variceal bleeding	33 (21.71)	18 (18.00)	15 (28.85)		
Refractory ascites	91 (59.87)	61 (61.00)	30 (57.69)		
Combined indications (bleeding and ascites)	28 (18.42)	21 (21.00)	7 (13.46)		
DM/n(%)				X^2 = 1.09	0.297
No	112 (73.68)	71 (71.00)	41 (78.85)		
Yes	40 (26.32)	29 (29.00)	11 (21.15)		
CHD/n(%)				X^2 = 0.00	1.000
No	143 (94.08)	94 (94.00)	49 (94.23)		
Yes	9 (5.92)	6 (6.00)	3 (5.77)		
Hypertension/n(%)				X^2 = 3.16	0.075
No	119 (78.29)	74 (74.00)	45 (86.54)		
Yes	33 (21.71)	26 (26.00)	7 (13.46)		
Child-Pugh grade/n(%)				X^2 = 7.78	0.020
A (scores 5–6)	44 (28.95)	36 (36.00)	8 (15.38)		
B (scores 7–9)	92 (60.53)	56 (56.00)	36 (69.23)		
C (scores 10–15)	16 (10.53)	8 (8.00)	8 (15.38)		
Child-Pugh score/[M (Q_1, Q_3)]	8.00 (6.00, 8.00)	7.00 (6.00, 8.00)	8.00 (7.00, 9.00)	Z = −1.81	0.070
MELD score/[M (Q_1, Q_3)]	9.0 (6.0, 11.0)	8.0 (5.0, 10.0)	11.0 (8.0, 12.0)	Z = −3.05	0.002
MELD-Na/[Mean ± SD]	10.0 (7.0, 12.0)	9.0 ± 4.0	12.0 ± 6.0	t = −3.17	0.002
MELD 3.0	11.0 (9.0, 14.0)	11.0 (9.0, 13.0)	12.0 (10.0, 15.0)	Z = −2.75	0.006
WBC/[×10^{12}/L, M (Q_1, Q_3)]	2.88 (2.25, 4.03)	2.96 (2.36, 4.47)	2.84 (2.01, 3.74)	Z = −1.40	0.16
Hemoglobin/[g/L, Mean ± SD]	88.91 ± 21.60	88.86 ± 22.01	89.00 ± 21.00	t = −0.04	0.97
Platelets/[×10^9/L, M (Q_1, Q_3)]	64.00 (44.75, 88.50)	74.50 (54.75, 97.00)	47.50 (38.75, 64.50)	Z = −4.58	<.001

(continued)

Table 1. *(continued)*

Variables	Total (n = 152)	Clinically stable group (n = 100)	Further decompensation group (n = 52)	Statistic	p
Albumin/[g/L, Mean ± SD]	33.97 ± 5.73	34.23 ± 5.99	33.47 ± 5.20	t = 0.78	0.435
ALT/[U/L, M (Q$_1$, Q$_3$)]	19.00 (13.00, 26.00)	19.00 (13.00, 26.00)	17.50 (13.50, 25.25)	Z = −0.71	0.479
AST/[U/L, M (Q$_1$, Q$_3$)]	26.50 (21.00, 37.10)	27.00 (23.00, 38.50)	24.50 (20.00, 37.00)	Z = −1.53	0.127
ALP/[U/L, M (Q$_1$, Q$_3$)]	87.50 (62.75, 118.25)	83.50 (65.00, 108.75)	92.50 (59.75, 128.50)	Z = −0.64	0.523
GGT/[U/L, M (Q$_1$, Q$_3$)]	34.50 (20.00, 66.00)	38.00 (22.75, 71.00)	31.00 (17.00, 58.25)	Z = −1.50	0.133
Total Bilirubin/[μmol/L,M (Q$_1$, Q$_3$)]	19.70 (14.88, 29.33)	18.15 (14.35, 24.88)	23.90 (17.38, 34.70)	Z = −2.61	0.009
PTA/[%, Mean ± SD]	70.78 ± 16.55	73.38 ± 16.42	65.77 ± 15.76	t = 2.75	0.007
Blood Glucose/[mmol/L, M (Q$_1$, Q$_3$)]	6.14 (5.23, 8.25)	6.20 (5.28, 8.56)	6.03 (5.11, 7.58)	Z = −0.77	0.444
Urea/[mmol/L, M (Q$_1$, Q$_3$)]	6.43 (4.42, 8.78)	6.27 (4.26, 8.38)	6.88 (4.63, 8.89)	Z = −1.04	0.301
Creatinine/[μmol/L, M (Q$_1$, Q$_3$)]	64.00 (54.00, 85.00)	63.00 (54.75, 83.00)	68.00 (53.75, 89.25)	Z = −0.58	0.564
Blood Ammonia/[μmol/L, M (Q$_1$, Q$_3$)]	33.00 (22.00, 48.50)	32.50 (21.50, 48.00)	38.50 (22.75, 51.00)	Z = −0.91	0.365
Follow-up duration/[months, M (Q$_1$, Q$_3$)]	12.0 (7.8, 12.0)	12.0 (12.0, 12.0)	3.8 (2.5, 8.2)	Z = −0.91	0.365

aOther causes included: cryptogenic cirrhosis (n = 26), nonalcoholic fatty liver disease cirrhosis (n = 4), drug-induced liver injury leading to cirrhosis (n = 2). Data are presented as mean ± standard deviation (SD) for normally distributed variables, median (Q$_1$, Q$_3$) for non-normally distributed variables, and n (%) for categorical variables. Statistical notations: t (Student's t-test), Z (Mann–Whitney U test), χ^2 (Chi-square test). AIH, autoimmune hepatitis; PBC, primary biliary cholangitis; DM, diabetes mellitus; CHD, coronary heart disease; MELD, model for end-stage liver disease; WBC, white blood cell count; ALT, alanine aminotransferase; AST, aspartate aminotransferase; ALP, alkaline phosphatase; GGT, gamma-glutamyl transferase; PTA, prothrombin time activity; Urea, urea nitrogen.

Table 2. Comparison of imaging indicators and TIPS hemodynamic parameters between the further decompensation group and the clinically stable group

Variables	Total (n = 152)	Clinically stable group (n = 100)	Further decompensation group (n = 52)	Statistic	p
Left hepatic lobe volume/[100 cm³, M (Q$_1$, Q$_3$)]	4.31 (3.40, 5.37)	4.51 (3.29, 5.46)	4.08 (3.48, 5.09)	Z = −0.61	0.541
Right hepatic lobe volume/[100 cm³, M (Q$_1$, Q$_3$)]	5.23 (4.18, 6.80)	5.39 (4.42, 7.30)	4.43 (3.57, 5.44)	Z = −3.50	<0.001
Caudate lobe volume/[100 cm³, M (Q$_1$, Q$_3$)]	0.26 (0.21, 0.36)	0.27 (0.21, 0.35)	0.24 (0.21, 0.37)	Z = −0.58	0.559
Spleen volume/[100 cm³, M (Q$_1$, Q$_3$)]	8.26 (5.82, 10.56)	7.26 (5.23, 9.23)	10.42 (8.92, 14.11)	Z = −6.04	<0.001
Pre-shunt PPG/[mmHg, Mean ± SD]	28.40 ± 5.36	27.74 ± 5.44	29.66 ± 5.02	t = −2.11	0.036
Post-shunt PPG/[mmHg, Mean ± SD]	10.57 ± 3.70	9.81 ± 3.80	12.02 ± 3.05	t = −3.62	<0.001
Reduction of PPG by TIPS/[(%), Mean ± SD]	62.62 ± 11.79	64.45 ± 12.29	59.08 ± 9.95	t = 2.91	<0.004
Spontaneous portosystemic shunt/n(%)				χ^2 = 1.23	0.267
No	108 (71.05)	74 (74.00)	34 (65.38)		
Yes	44 (28.95)	26 (26.00)	18 (34.62)		
Portal vein thrombosis/n(%)				χ^2 = 1.48	0.224
No	92 (60.53)	64 (64.00)	28 (53.85)		
Ye	60 (39.47)	36 (36.00)	24 (46.15)		
Portal vein cavernous transformation/n(%)				χ^2 = 0.15	0.694
No	146 (96.05)	97 (97.00)	49 (94.23)		
Yes	6 (3.95)	3 (3.00)	3 (5.77)		

Data are presented as mean ± standard deviation (SD) for normally distributed variables, median (Q$_1$, Q$_3$) for non-normally distributed variables, and n (%) for categorical variables. Statistical notations: t (Student's t-test), Z (Mann–Whitney U test), χ^2 (Chi-square test). PP, portal pressure; PPG, portal pressure gradient; IVC, inferior vena cava pressure; PPG, portal pressure gradient.
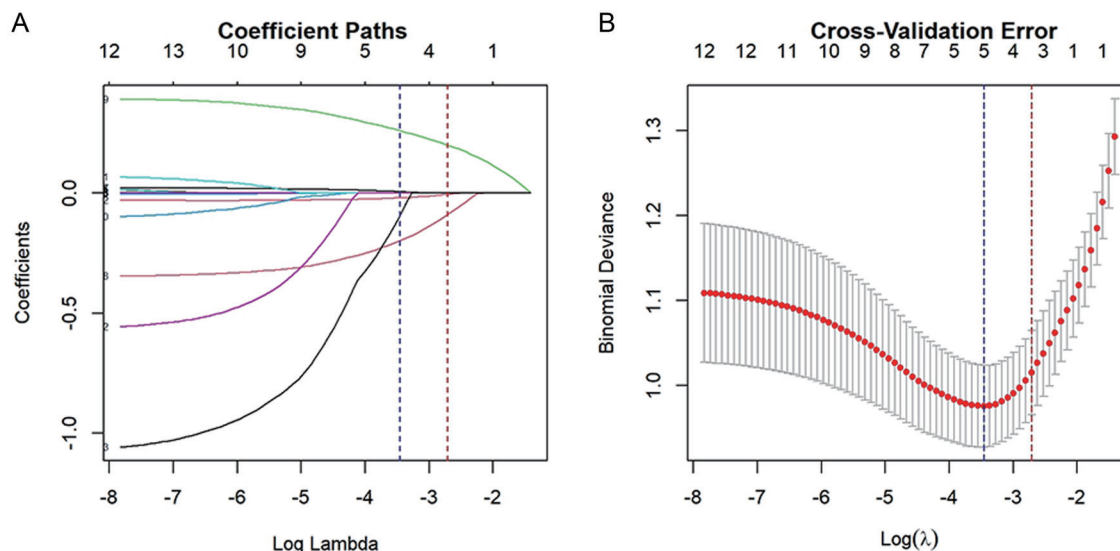
Fig. 3. Predictive Variables Selected by Lasso Regression Model. (A) Coefficient trajectories of candidate variables across varying penalty parameters (λ) in Lasso regression. (B) Optimal feature selection through 10-fold cross-validation in the Lasso regression model.

Risk factor selection and power analysis for further decompensation within one year post-TIPS: Univariable, LASSO regression, and post hoc assessment

Univariable logistic regression ($p < 0.10$ threshold) identified 11 candidate predictors for one-year post-TIPS decompensation (Supplementary Table 3). Given the potential clinical relevance of TIPS indication, particularly the trend toward reduced further decompensation risk observed in combined indications (bleeding and ascites) versus variceal bleeding alone (OR 0.40, 95% CI 0.13–1.20, $p = 0.101$), this variable was added to LASSO regression. Due to significant collinearity between post-shunt PPG and PPG reduction (Pearson's r = 0.820, $p < 0.001$), versus nonsignificant correlation between pre-shunt PPG and PPG reduction (r = 0.078, $p = 0.339$) (Supplementary Fig. 1), post-shunt PPG was excluded. LASSO regression with 10-fold cross-validation (optimal λ = 0.066) selected three predictors: right hepatic lobe volume, spleen volume, and PPG reduction (Fig. 3); notably, all TIPS indication categories were excluded by the λ-1se criterion.

The λ-1se model (AUC = 0.854) demonstrated comparable performance to λ-min (AUC = 0.865) but improved simplicity, thus retained for final analysis. Post hoc power analysis of these final predictors revealed: 99.9% power for spleen volume, 79.2% for hepatic volume, and 21.6% for PPG reduction, aligning with their respective OR magnitudes.

Nomogram development and validation for post-TIPS one-year further decompensation risk

Multivariable analysis confirmed independent associations of right hepatic lobe volume (OR = 0.683, 95% CI = 0.535–0.873), spleen volume (OR = 1.435, 95% CI = 1.240–1.661), and PPG reduction (OR = 0.961, 95% CI = 0.927–0.996) with post-TIPS further decompensation (all $p < 0.05$) (Supplementary Table 4). A 100 cm^3 increase in right hepatic lobe volume reduced risk by 31.7%, whereas equivalent spleen volume expansion increased risk by 43.5%; each 1% PPG reduction decreased risk by 3.9%.

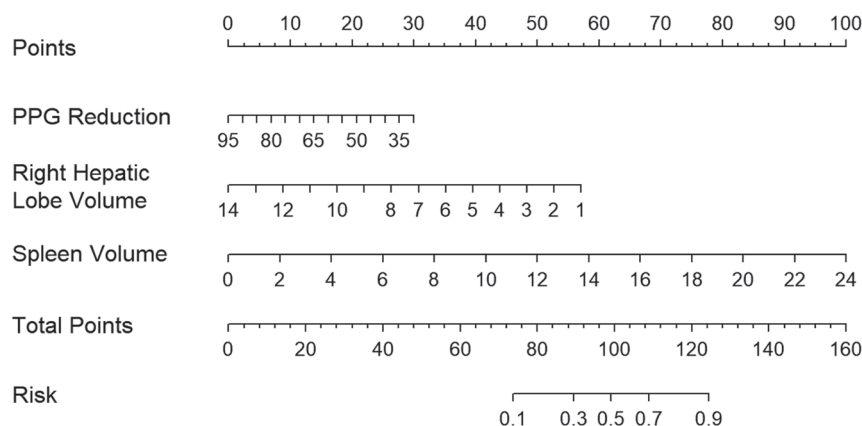The nomogram (Fig. 4) demonstrated discriminative ca-

Fig. 4. Nomogram for predicting the risk of further decompensation within one year after TIPS in patients with decompensated cirrhosis. Sum points for PPG reduction, right hepatic lobe volume, and spleen volume to calculate total points; draw a vertical line from the total points axis to the risk axis to determine the probability of further decompensation within one year. Further decompensation risk score = −4.39 × (right hepatic lobe volume) + 4.17 × (spleen volume) - 0.46 × (PPG reduction) + 105.21. TIPS, transjugular intrahepatic portosystemic shunt; PPG, portal pressure gradient.
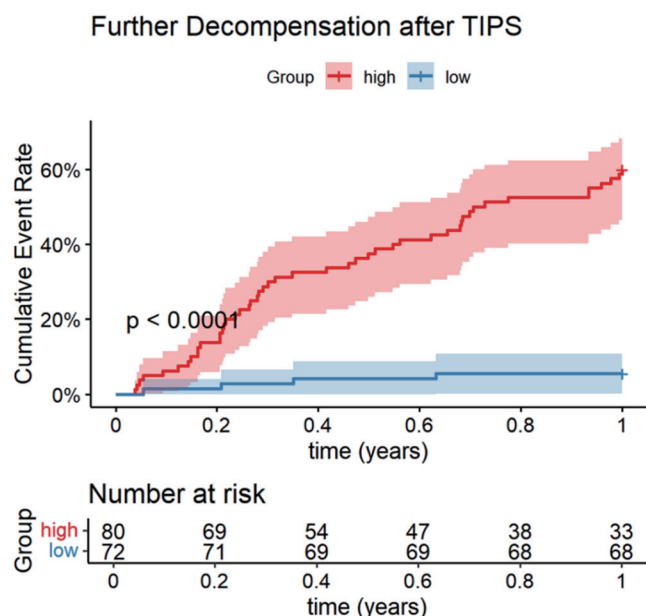
Further Decompensation after TIPS

Fig. 5. Cumulative probability of further decompensation within one year after TIPS stratified by nomogram model cut-off scores. High: nomogram model scores > 86 points, low: nomogram model scores ≤ 86 points. Patients scoring >86 points (high-risk group) had a 10.7-fold increased risk of further decompensation within one year compared to those scoring ≤86 points (low-risk group) (*p* < 0.001 by log-rank test). TIPS, transjugular intrahepatic portosystemic shunt.

pacity (AUC = 0.854, 95% CI = 0.792–0.915; Supplementary Fig. 2) with sensitivity = 92.3% and specificity = 68.0%. Bootstrap validation (1,000 resamples) confirmed discriminative ability (AUC = 0.784), calibration (Hosmer-Lemeshow χ^2 = 13.053, *p* = 0.110; MAE = 0.035; Supplementary Fig. 3), and clinical utility (net benefit across 10%–90% thresholds; Supplementary Fig. 4).

Compared to PPG reduction and benchmark prognostic scores, the model showed superior AUC: +0.229 vs. PPG reduction alone (0.625 vs. 0.854; DeLong's *p* < 0.001), +0.235 vs. Child-Pugh (0.619 vs. 0.854; *p* < 0.001), +0.201 vs. MELD (0.653 vs. 0.854; *p* < 0.001), +0.202 vs. MELD-Na (0.652 vs. 0.854; *p* < 0.001), and +0.223 vs. MELD 3.0 (0.631 vs. 0.854; *p* < 0.001) (Supplementary Fig. 5, Supplementary Table 5).

Validation of KM curves for a predictive model of the risk of further decompensation at one year after TIPS

The ROC-derived optimal risk cutoff of 86 points (AUC = 0.854, 95% CI = 0.792–0.915) stratified patients into high- (n = 80, > 86) and low-risk (n = 72, ≤86) groups. Score distribution analysis revealed distinct patterns: low-risk scores clustered at 40–80 (peak = 20 cases), while high-risk scores exceeded 80 (100%) (Supplementary Fig. 6). High-risk patients had higher one-year decompensation rates (60.0% vs 5.6%, *p* < 0.001) and cumulative risk (HR = 15.03, 95% CI = 8.70–25.98; Log-rank *p* < 0.0001; Fig. 5, Supplementary Table 6). The model quantifies high-risk features (reduced right hepatic lobe volume, splenomegaly, limited PPG reduction), guiding prioritized post-TIPS interventions and individualized management. Using the ROC-derived cutoff (86 points), we implemented a publicly available web calculator (https://doi.org/10.5281/zenodo.16619257; operational: https://post-tips.shinyapps.io/Post-TIPS/) with an interface

shown in Supplementary Figure 7.

Sensitivity analysis excluding patients with early HE

Sensitivity analyses excluding early HE (≤90 days post-TIPS, n = 5) demonstrated minimal absolute changes in predictor effect sizes: right hepatic lobe volume (ΔOR = +0.020, Pinteraction = 0.874), spleen volume (ΔOR = +0.039, Pinteraction = 0.808), and PPG reduction (ΔOR = −0.004, Pinteraction = 0.891), with non-significant improvement in model discrimination (ΔAUC = 0.016, DeLong's *p* = 0.711) (Supplementary Table 7).

Subgroup analysis of etiology, etiology-specific therapy, and first decompensation events

Analysis across etiological subgroups (viral, alcohol-associated, primary biliary cholangitis, autoimmune, other) revealed no significant differences in spleen volume (*p* = 0.117), PPG reduction (*p* = 0.263), and further decompensation incidence (*p* = 0.608) (Supplementary Table 8). However, baseline right hepatic lobe volume differed significantly (*p* < 0.001), with alcohol-associated cirrhosis patients exhibiting larger volumes (median 7.09 × 100 cm³; IQR 5.71–9.77 cm³).

In elimination-amenable etiologies, treated cohorts exhibited post-TIPS further decompensation rates of 39.47% for antiviral-treated HBV (n = 38), 42.86% for antiviral-treated HCV (n = 7), and 25.00% for abstinent alcohol-associated cirrhosis (n = 20). The addition of etiology-specific therapy resulted in minimal perturbation of core predictors (max ΔOR = 0.003) without significant discrimination improvement (ΔAUC = 0.003, DeLong's *p* = 0.19). Complete outcomes are in Supplementary Table 9 and model metrics in Supplementary Table 10.

Analysis of first decompensation events revealed no significant differences between the PHE (n = 38) and HE (n = 14) groups in right hepatic lobe volume (median 4.7 cm³ vs. 3.85 × 100 cm³, *p* = 0.247), spleen volume (median 10.85 cm³ vs. 9.58 × 100 cm³, *p* = 0.101), or PPG reduction (58.39% ± 10.04% vs. 60.98% ± 9.83%, *p* = 0.411) (Supplementary Table 11).

Discussion

Hepatic decompensation constitutes a pivotal clinical event in cirrhosis progression, profoundly impacting patient outcomes.[22] The latest consensus defines decompensation as the onset of overt portal hypertension-related complications, particularly refractory ascites, variceal hemorrhage, or overt HE.[23] Cirrhosis naturally progresses from a compensated state to decompensation, often followed by recurrent decompensation events.[24] While median survival exceeds 12 years in treated compensated patients, this drops to <1.5 years post-decompensation.[23] Approximately 60% of decompensated patients experience further decompensation episodes without intervention, significantly elevating mortality.[25] A PREDICT study stratified one-year mortality as 9.5% vs. 35.6% in stable vs. unstable decompensated cohorts.[26] Consequently, mitigating further decompensation is paramount for reducing hospitalization and mortality risks.[27,28] Etiology-targeted interventions (e.g., antiviral therapy for viral hepatitis, alcohol cessation) may achieve recompensation in select patients.[29] TIPS, by reducing PP through intrahepatic portocaval shunting, demonstrates similar recompensation potential. Meta-analytic evidence demonstrates that TIPS placement confers a 44% reduction in further decompensation risk across etiologies compared to conventional medical therapy.[1] Our findings corroborate this therapeutic

efficacy, with 65.79% of patients maintaining clinical stability and 35.92% attaining hepatic recompensation within one year post-TIPS (unpublished observations), validating TIPS as an effective intervention for promoting hepatic recompensation. However, therapeutic responses vary among patients with cirrhosis undergoing TIPS. Our cohort analysis found that 34.2% (52/152) experienced further decompensation post-TIPS. This underscores the critical need for preoperative risk stratification to guide personalized intervention strategies and implement targeted preventive measures against decompensation recurrence.

Current investigations into predictors of further hepatic decompensation post-TIPS remain limited.[6] Sturm *et al*.[6] demonstrated that the Freiburg index of post-TIPS survival, incorporating age, serum creatinine, bilirubin, and albumin, predicts further decompensation. Furthermore, their finding that TIPS indications lack independent prognostic value aligns with our results. Critically, this study is the first to validate the independent predictive value of right hepatic lobe volume (OR = 0.683), spleen volume (OR = 1.435), and PPG reduction (OR = 0.961) for post-TIPS further decompensation. Integration of these parameters yielded a nomogram model with discriminative capacity (AUC = 0.854), providing radiologically grounded criteria for preoperative identification of TIPS candidates most likely to achieve clinical benefit.

Hepatic and splenic volumetry quantifies parenchymal changes in cirrhosis and serves as validated biomarkers of disease severity.[30] Our volumetric methodology showed excellent measurement precision (ICC > 0.950 for liver lobes/total liver; ICC = 0.982 for spleen), while Bland-Altman results reflect biological variability. Splenomegaly, driven by portal hypertension-induced splenic venous congestion,[9,31] constitutes an established prognostic predictor.[9] Consistent with multicenter evidence demonstrating 3D hepatic/splenic morphometry predicts overt HE post-TIPS,[3] our findings identify spleen volume as an independent risk factor for further decompensation (OR = 1.435), with each 100 cm^3 increment elevating risk by 43.5%. Hepatic volumetry reflects functional reserve through viable hepatocyte mass quantification,[10] paralleling observations by Patel *et al*.[32] of reduced total/functional liver volumes and increased spleen volumes in decompensated cirrhosis. A cross-sectional study[33] revealed segment-specific volumetric alterations in patients with cirrhosis, demonstrating relative atrophy of the right lobe and medial sector of the left lobe (Couinaud segments IV-VIII) alongside hypertrophy of the left lateral sector and caudate lobe (segments I-III). However, the prognostic implications of lobar volumetric changes for post-TIPS further decompensation remain underexplored. We investigated associations between hepatic lobar volumetry and post-TIPS further decompensation risk. Notably, right hepatic lobe volume emerged as a protective factor against one-year decompensation (OR = 0.683, 95% CI 0.535–0.873), with each 100 cm^3 increment conferring a 31.7% risk reduction. In contrast, left lobe and caudate lobe volumes showed no significant associations, possibly due to limited sample size and lack of subsegmental left lobe analysis. Given that measurement precision ensures anatomical capture (ICC > 0.95) and observed biological variations are clinically insignificant, single-timepoint assessment provides valid baseline data for pre-TIPS planning without repeat imaging.

Complementing these anatomical predictors, dynamic monitoring of PPG holds critical prognostic value in patients with cirrhosis and portal hypertension.[34] Per the Baveno VII consensus, post-shunt PPG thresholds (<12 mmHg absolute value; >50% relative reduction) are established therapeutic targets for preventing variceal rebleeding.[2] Notably, emerging evidence associates the magnitude of PPG reduction with post-TIPS decompensation risk. Queck *et al*.[35] demonstrated that <60% PPG reduction significantly correlates with refractory ascites development within six weeks post-TIPS. However, the prognostic value of PPG reduction for post-TIPS further decompensation was unclear. We found significant collinearity between post-shunt PPG and PPG reduction magnitude (Pearson's r = 0.82, *p* < 0.001). PPG reduction was prioritized as the core predictor given its superior sensitivity in quantifying the hemodynamic response to shunt creation. This selection was substantiated by two key pieces of evidence: (1) The absence of a significant correlation between pre-shunt and PPG reduction (Pearson's r = 0.078, *p* = 0.339), suggesting limited predictability of post-shunt hemodynamic changes by pre-shunt PP levels; (2) PPG reduction integrates pre- and post-procedural pressure dynamics and avoids multicollinearity problems from using isolated post-shunt PPG. Notably, our results demonstrated that each 1% increase in PPG reduction decreased further decompensation risk by 3.9%, confirming the prognostic value of monitoring PPG changes.

Power analysis of this model revealed distinct clinical implications: Spleen volume's near-perfect power (>99.9%) confirms it as a robust predictor of post-TIPS further decompensation. Hepatic volume's 79.2% power—supported by its substantial protective effect (31.7% risk reduction per unit) and biological plausibility in liver reserve assessment—remains clinically actionable despite conventional 80% thresholds. For PPG reduction (a Baveno VII-endorsed hemodynamic target[2]), the 21.6% power reflects its modest effect size (3.9% risk reduction per unit) rather than clinical irrelevance. Its inclusion preserves the physiological completeness of the model.

The relatively low HBV-related cirrhosis proportion (28.94%) aligns with recent Chinese data,[3] likely reflecting antiviral therapy's effectiveness in preventing decompensation. Diverging from prior reports, age, bilirubin, and albumin showed no significant associations with post-TIPS further decompensation in our cohort. This discrepancy may be attributable to: (1) Population heterogeneity—HBV-related cirrhosis predominance (58.55%) versus alcohol-associated cohorts in previous reports; (2) Adjustment for strong confounders: Including robust predictors (right hepatic lobe/spleen volumetry) may have masked associations of conventional biomarkers; (3) Sample size limitations: Although the cohort size (n = 152) met basic analytical requirements, statistical power for subgroup analyses remained suboptimal—exemplified by elderly patients (>65 years) constituting only 28.95% of the cohort, potentially obscuring age-related associations. These discrepancies suggest that the generalizability of post-TIPS risk factors may be influenced by population characteristics and study design, necessitating validation through multicenter, large-scale studies with enhanced subgroup representation.

This study optimized conventional modeling approaches through sequential univariable logistic regression, LASSO regularization, and multivariable logistic regression. LASSO's regularization mechanism effectively prioritized variables with multidimensional predictive contributions while reducing overfitting, generating a parsimonious yet generalizable model.[36] The λ-1se criterion was selected over λ-min to balance model complexity and clinical utility. Critically, the λ-1se LASSO objectively excluded TIPS indication variables while retaining right hepatic lobe volume, spleen volume, and PPG reduction—all independently significant predictors (*p* < 0.05) in multivariable analysis. This aligns with the known pathophysiology of post-TIPS decompensation. The resultant nom-

ogram integrates statistical rigor with clinical interpretability, offering a streamlined tool for risk stratification in TIPS clinical decision-making.

The nomogram integrating hepatosplenic volumetry and hemodynamic profiling (PPG reduction) had excellent discrimination (AUC 0.854) and precise calibration (MAE 0.035). Bootstrap validation confirmed generalizability (AUC 0.784, Brier 0.180), while decision curve analysis demonstrated clinical utility across risk thresholds. Critically, the absence of TIPS thrombosis-related decompensation indicates that observed decompensation events primarily reflect progressive hepatic dysfunction. This aligns with contemporary studies reporting low annual thrombosis rates (≤6%) in covered stents,[37] confirming that our nomogram specifically predicts the risk of hepato-functional decompensation, not decompensation due to stent thrombosis. Furthermore, our composite model outperformed both benchmark prognostic scores (Child-Pugh, MELD, MELD-Na, MELD 3.0) and the isolated hemodynamic parameter (PPG reduction). Benchmark predictive scores rely exclusively on static serum biomarkers (e.g., bilirubin, INR) or electrolyte parameters (sodium). While PPG reduction can directly measure PP, it provides merely a cross-sectional hemodynamic snapshot. Neither approach fully captures cumulative hepatosplenic damage from chronic portal hypertension. Our model quantifies this through integrated morphometric proxies (right liver atrophy, splenomegaly) and hemodynamic indicators (PPG reduction). Survival analysis based on the nomogram-derived cutoff (86 points) revealed significantly elevated decompensation risk in high-score patients. The visual scoring system enhances clinical utility by explicitly quantifying risk contributors, enabling personalized postoperative risk stratification.

To enhance model generalizability, our cohort incorporated patients with cirrhosis of heterogeneous etiologies, aligning with established volume-related research methods in portal hypertension research.[3,12,38] While the model demonstrated robust overall performance, subgroup analyses revealed etiology-specific morphological variation: patients with alcohol-associated cirrhosis exhibited significantly larger baseline right hepatic lobe volumes than those with other etiologies, consistent with the findings of Kim *et al*.[39] This likely reflects characteristic dual pathophysiological mechanisms in alcohol-related injury: hepatic steatosis-induced hypertrophy and asymmetric fibrotic remodeling.[40,41] Crucially, core predictors beyond hepatic volumetry—PPG reduction and spleen volume—remained etiology-agnostic across subgroups, supporting their utility as universal hemodynamic and portal hypertension severity markers. When applying this model to populations with markedly different etiology distributions, such as cohorts with predominantly alcohol-associated cirrhosis, external validation in diverse populations is essential. Beyond these etiology-driven morphological variations, the model demonstrated invariant robustness to therapeutic heterogeneity. Despite descriptive variations in etiology-specific decompensation rates, our predictive model maintained robustness when adjusted for elimination-amenable therapies. The maximal effect size perturbation was ≤0.003 OR units with a non-significant discrimination change (*p* = 0.19), mechanistically affirming the stability of the nomogram across therapeutic heterogeneity. Additionally, baseline levels of key volumetric (hepatic/splenic) and hemodynamic (PPG reduction) predictors showed no significant differences between decompensation phenotypes (PHE vs. HE) in the overall cohort. Although the subanalysis comparing first decompensation events (PHE, n = 38; HE, n = 14) was statistically underpowered due to the limited HE sample size, directionally consistent trends suggested smaller hepatic volumes, reduced splenic volumes, and greater PPG reduction in the HE group. Nevertheless, the consistent absence of statistical significance across all analyses (all *p* > 0.10) confirms that these core predictors operate independently of decompensation phenotype. This supports their integration into a unified predictive model for post-TIPS further decompensation risk, regardless of initial clinical presentation. Furthermore, sensitivity analyses excluding early HE demonstrated minimal effect size perturbations (max ΔOR = 0.039) with preserved discrimination (ΔAUC = 0.016, *p* = 0.711). These findings substantiate that liver/spleen volumetry primarily reflects disease progression rather than TIPS procedure-related complications. The stability of predictor effects supports the model's applicability in broader patient cohorts, including those with early HE.

The study presents two key innovations: First, for the first time, right hepatic lobe volume, spleen volume, and PPG reduction were identified as independent predictors of further decompensation within one year after TIPS in patients with decompensated cirrhosis. Second, the development of a novel nomogram integrating hepatosplenic volumetry and hemodynamic parameters with superior predictive accuracy (AUC = 0.854). Three principal limitations warrant consideration: First, this single-center retrospective design using an HBV-predominant Chinese cohort may limit generalizability. Future multi-center external validation in cohorts encompassing different etiologies of cirrhosis (e.g., alcohol-related liver disease, non-alcoholic fatty liver disease) and geographically/ethnically diverse populations is essential. Second, although 3D Slicer enables semi-automated volumetry, the process remains time-consuming, requires specialized training, and introduces inter-observer variability during manual adjustments. This underscores the critical need for fully automated tools. Future integration of validated AI-based algorithms with Picture Archiving and Communication Systems is crucial to eliminate observer dependency and facilitate clinical implementation. Third, the small subgroup sizes for rare etiologies (e.g., primary biliary cholangitis, n = 14) and for patients lacking etiology-specific therapies (e.g., untreated HBV, n = 6) limited statistical power. Future multi-center studies with larger cohorts should incorporate stratification by etiology and treatment exposure to validate the broader applicability of the model. Despite these limitations, this model enables early identification of high-risk patients through a freely accessible web calculator, which provides instantaneous risk quantification using the nomogram-derived formula. This tool facilitates personalized surveillance protocols and therapeutic adjustments that may ultimately improve clinical outcomes through enhanced survival rates and reduced healthcare/societal burdens. The semi-automated visceral volumetry approach presented here provides a practical foundation for developing AI-based prognostic tools.

Conclusions

In summary, 34.2% of decompensated patients with cirrhosis experience further decompensation post-TIPS, despite improved outcomes in most. Right hepatic lobe volume and post-shunt PPG reduction were identified as protective factors against one-year further decompensation, whereas spleen volume emerged as an independent risk factor. The nomogram model constructed based on these indicators demonstrated promising discriminative accuracy in stratifying patients with decompensated cirrhosis who are at high risk of post-TIPS further decompensation, serving as an evidence-based decision-support tool to guide therapeutic selection, risk quantification, and personalized management.

Conflict of interest

The authors have no conflicts of interest related to this publication.

Author contributions

Study design (XC, HX, YL, QY), performance of experiments (XC, YL, FL), analysis and interpretation of data (XC, LJ, YZ, KJ, JT, RL, NW, WY, FW, PZ), manuscript writing (XC, CY, ZG, JW, TW), critical revision (HX, YL, QY), statistical analysis (XC, JY, YL), and critical funding (HX). All authors reviewed and commented on the manuscript. All authors approved the final manuscript.

Ethical statement

This study protocol conforms to the ethical guidelines of the 2024 Declaration of Helsinki. This study was approved by the Ethics Committee of Tianjin Third Central Hospital (IRB2019-022-04). The individual consent for this retrospective analysis was waived.

Data sharing statement

The datasets generated during and/or analyzed during the current study are available from the corresponding author upon reasonable request.

References

[1] Larrue H, D'Amico G, Olivas P, Lv Y, Bucsics T, Rudler M, *et al*. TIPS prevents further decompensation and improves survival in patients with cirrhosis and portal hypertension in an individual patient data meta-analysis. J Hepatol 2023;79(3):692–703. doi:10.1016/j.jhep.2023.04.028, PMID:37141993.

[2] de Franchis R, Bosch J, Garcia-Tsao G, Reiberger T, Ripoll C, Baveno VII Faculty. Baveno VII - Renewing consensus in portal hypertension. J Hepatol 2022;76(4):959–974. doi:10.1016/j.jhep.2021.12.022, PMID:35120736.

[3] Chen X, Wang T, Ji Z, Luo J, Lv W, Wang H, *et al*. 3D automatic liver and spleen assessment in predicting overt hepatic encephalopathy before TIPS: a multi-center study. Hepatol Int 2023;17(6):1545–1556. doi:10.1007/s12072-023-10570-5, PMID:37531069.

[4] Tripathi D, Stanley AJ, Hayes PC, Travis S, Armstrong MJ, Tsochatzis EA, *et al*. Transjugular intrahepatic portosystemic stent-shunt in the management of portal hypertension. Gut 2020;69(7):1173–1192. doi:10.1136/gutjnl-2019-320221, PMID:32114503.

[5] Yang C, Chen Q, Zhou C, Liu J, Huang S, Wang Y, *et al*. FIPS Score for Prediction of Survival After TIPS Placement: External Validation and Comparison With Traditional Risk Scores in a Cohort of Chinese Patients With Cirrhosis. AJR Am J Roentgenol 2022;219(2):255–267. doi:10.2214/AJR.21.27301, PMID:35138134.

[6] Sturm L, Schultheiss M, Stöhr F, Labenz C, Maasoumy B, Tiede A, *et al*. Freiburg index of post-TIPS survival (FIPS) identifies patients at risk of further decompensation and ACLF after TIPS. J Hepatol 2025;83(2):348–357. doi:10.1016/j.jhep.2025.01.030, PMID:39914747.

[7] Zhang W, Jin YN, Sun C, Zhang XF, Li RQ, Yin Q, *et al*. Development and validation of a predictive model for acute-on-chronic liver failure after transjugular intrahepatic portosystemic shunt. World J Gastrointest Surg 2024;16(5):1301–1310. doi:10.4240/wjgs.v16.i5.1301, PMID:38817303.

[8] Kutaiba N, Chung W, Goodwin M, Testro A, Egan G, Lim R. The impact of hepatic and splenic volumetric assessment in imaging for chronic liver disease: a narrative review. Insights Imaging 2024;15(1):146. doi:10.1186/s13244-024-01727-3, PMID:38886297.

[9] Wang P, Hu X, Xie F. Predictive value of liver and spleen stiffness measurement based on two-dimensional shear wave elastography for the portal vein pressure in patients with compensatory viral cirrhosis. PeerJ 2023;11:e15956. doi:10.7717/peerj.15956, PMID:37727690.

[10] Hu C, Jiang N, Zheng J, Li C, Huang H, Li J, *et al*. Liver volume based prediction model for patients with hepatitis B virus-related acute-on-chronic liver failure. J Hepatobiliary Pancreat Sci 2022;29(12):1253–1263. doi:10.1002/jhbp.1112, PMID:35029044.

[11] Kwon JH, Lee SS, Yoon JS, Suk HI, Sung YS, Kim HS, *et al*. Liver-to-Spleen Volume Ratio Automatically Measured on CT Predicts Decompensation in Patients with B Viral Compensated Cirrhosis. Korean J Radiol 2021;22(12):1985–1995. doi:10.3348/kjr.2021.0348, PMID:34564961.

[12] Iranmanesh P, Vazquez O, Terraz S, Majno P, Spahr L, Poncet A, *et al*. Accurate computed tomography-based portal pressure assessment in patients with hepatocellular carcinoma. J Hepatol 2014;60(5):969–974. doi:10.1016/j.jhep.2013.12.015, PMID:24362073.

[13] Sanyal AJ, Freedman AM, Shiffman ML, Purdum PP 3rd, Luketic VA, Cheatham AK. Portosystemic encephalopathy after transjugular intrahepatic portosystemic shunt: results of a prospective controlled study. Hepatology 1994;20(1 Pt 1):46–55. doi:10.1016/0270-9139(94)90133-3, PMID:8020904.

[14] Iwakiri Y, Trebicka J. Portal hypertension in cirrhosis: Pathophysiological mechanisms and therapy. JHEP Rep 2021;3(4):100316. doi:10.1016/j.jhep.2021.100316, PMID:34337369.

[15] Arnold J, Avila E, Idalsoaga F, Diaz LA, Ayala Valverde M, Ayares G, *et al*. Advances in the diagnosis and management of hepatorenal syndrome: insights into HRS-AKI and liver transplantation. eGastroenterology 2023;1(2):e100009. doi:10.1136/egastro-2023-100009, PMID:39943997.

[16] Chinese Society of Hepatology,Chinese Medical Association. [Chinese guidelines on the management of liver cirrhosis]. Zhonghua Gan Zang Bing Za Zhi 2019;27(11):846–865. doi:10.3760/cma.j.issn.1007-3418.2019.11.008.

[17] Reau NS, Lammert CS, Weinberg EM. Autoimmune hepatitis: Current and future therapies. Hepatol Commun 2024;8(6):e0458. doi:10.1097/HC9.0000000000000458, PMID:38836863.

[18] Thüring J, Rippel O, Haarburger C, Merhof D, Schad P, Bruners P, *et al*. Multiphase CT-based prediction of Child-Pugh classification: a machine learning approach. Eur Radiol Exp 2020;4(1):20. doi:10.1186/s41747-020-00148-3, PMID:32249336.

[19] Wiesner R, Edwards E, Freeman R, Harper A, Kim R, Kamath P, *et al*. Model for end-stage liver disease (MELD) and allocation of donor livers. Gastroenterology 2003;124(1):91–96. doi:10.1053/gast.2003.50016, PMID:12512033.

[20] Kim WR, Mannalithara A, Heimbach JK, Kamath PS, Asrani SK, Biggins SW, *et al*. MELD 3.0: The Model for End-Stage Liver Disease Updated for the Modern Era. Gastroenterology 2021;161(6):1887–1895.e4. doi:10.1053/j.gastro.2021.08.050, PMID:34481845.

[21] Wang M, Jin R, Lu J, Song E, Ma G. Automatic CT liver Couinaud segmentation based on key bifurcation detection with attentive residual hourglass-based cascaded network. Comput Biol Med 2022;144:105363. doi:10.1016/j.compbiomed.2022.105363, PMID:35290810.

[22] D'Amico G, Bernardi M, Angeli P. Towards a new definition of decompensated cirrhosis. J Hepatol 2022;76(1):202–207. doi:10.1016/j.jhep.2021.06.018, PMID:34157322.

[23] Kaplan DE, Ripoll C, Thiele M, Fortune BE, Simonetto DA, Garcia-Tsao G, *et al*. AASLD Practice Guidance on risk stratification and management of portal hypertension and varices in cirrhosis. Hepatology 2024;79(5):1180–1211. doi:10.1097/HEP.0000000000000647, PMID:37870298.

[24] Jalan R, D'Amico G, Trebicka J, Moreau R, Angeli P, Arroyo V. New clinical and pathophysiological perspectives defining the trajectory of cirrhosis. J Hepatol 2021;75(Suppl 1):S14–S26. doi:10.1016/j.jhep.2021.01.018, PMID:34039485.

[25] D'Amico G, Zipprich A, Villanueva C, Sordà JA, Morillas RM, Garcovich M, *et al*. Further decompensation in cirrhosis: Results of a large multicenter cohort study supporting Baveno VII statements. Hepatology 2024;79(4):869–881. doi:10.1097/HEP.0000000000000652, PMID:37916970.

[26] Trebicka J, Fernandez J, Papp M, Caraceni P, Laleman W, Gambino C, *et al*. The PREDICT study uncovers three clinical courses of acutely decompensated cirrhosis that have distinct pathophysiology. J Hepatol 2020;73(4):842–854. doi:10.1016/j.jhep.2020.06.013, PMID:32673741.

[27] García-Pagán JC, Caca K, Bureau C, Laleman W, Appenrodt B, Luca A, *et al*. Early use of TIPS in patients with cirrhosis and variceal bleeding. N Engl J Med 2010;362(25):2370–2379. doi:10.1056/NEJMoa0910102, PMID:20573925.

[28] Bureau C, Thabut D, Oberti F, Dharancy S, Carbonell N, Bouvier A, *et al*. Transjugular Intrahepatic Portosystemic Shunts With Covered Stents Increase Transplant-Free Survival of Patients With Cirrhosis and Recurrent Ascites. Gastroenterology 2017;152(1):157–163. doi:10.1053/j.gastro.2016.09.016, PMID:27663604.

[29] Wang Q, Zhao H, Deng Y, Zheng H, Xiang H, Nan Y, *et al*. Validation of Baveno VII criteria for recompensation in entecavir-treated patients with hepatitis B-related decompensated cirrhosis. J Hepatol 2022;77(6):1564–1572. doi:10.1016/j.jhep.2022.07.037, PMID:36038017.

[30] Etzion O, Takyar V, Novack V, Gharib AM, Canales R, Adebogun A, *et al*. Spleen and Liver Volumetrics as Surrogate Markers of Hepatic Venous Pressure Gradient in Patients With Noncirrhotic Portal Hypertension. Hepatol Commun 2018;2(8):919–928. doi:10.1002/hep4.1198, PMID:30094403.

[31] Helgesson S, Tarai S, Langner T, Ahlström H, Johansson L, Kullberg J, *et*

al. Spleen volume is independently associated with non-alcoholic fatty liver disease, liver volume and liver fibrosis. Heliyon 2024;10(8):e28123. doi:10.1016/j.heliyon.2024.e28123, PMID:38665588.

[32] Patel M, Tann M, Liangpunsakul S. CT-scan Based Liver and Spleen Volume Measurement as a Prognostic Indicator for Patients with Cirrhosis. Am J Med Sci 2021;362(3):252–259. doi:10.1016/j.amjms.2020.10.031, PMID:33947583.

[33] Romero-Cristóbal M, Clemente-Sánchez A, Peligros MI, Ramón E, Matilla AM, Colón A, *et al*. Liver and spleen volumes are associated with prognosis of compensated and decompensated cirrhosis and parallel its natural history. United European Gastroenterol J 2022;10(8):805–816. doi:10.1002/ueg2.12301, PMID:36065767.

[34] Qi X, Berzigotti A, Cardenas A, Sarin SK. Emerging non-invasive approaches for diagnosis and monitoring of portal hypertension. Lancet Gastroenterol Hepatol 2018;3(10):708–719. doi:10.1016/S2468-1253(18)30232-2, PMID:30215362.

[35] Queck A, Schwierz L, Gu W, Ferstl PG, Jansen C, Uschner FE, *et al*. Targeted decrease of portal hepatic pressure gradient improves ascites control after TIPS. Hepatology 2023;77(2):466–475. doi:10.1002/hep.32676, PMID:35869810.

[36] Tibshirani R. Regression Shrinkage and Selection Via the Lasso. Journal of the Royal Statistical Society: Series B (Methodological) 2018;58(1):267–

288. doi:10.1111/j.2517-6161.1996.tb02080.x.

[37] Jahangiri Y, Kerrigan T, Li L, Prosser D, Brar A, Righetti J, *et al*. Risk factors for stent graft thrombosis after transjugular intrahepatic portosystemic shunt creation. Cardiovasc Diagn Ther 2017;7(Suppl 3):S150–S158. doi:10.21037/cdt.2017.10.03, PMID:29399518.

[38] Romero-Cristóbal M, Clemente-Sánchez A, Ramón E, Téllez L, Canales E, Ortega-Lobete O, *et al*. CT-derived liver and spleen volume accurately diagnose clinically significant portal hypertension in patients with hepatocellular carcinoma. JHEP Rep 2023;5(3):100645. doi:10.1016/j.jhepr.2022.100645, PMID:36691569.

[39] Kim I, Jang YJ, Ryeom H, Lee SM, Lee HJ, Kim GC, *et al*. Variation in hepatic segmental volume distribution according to different causes of liver cirrhosis: CT volumetric evaluation. J Comput Assist Tomogr 2012;36(2):220–225. doi:10.1097/RCT.0b013e31824afd86, PMID:22446363.

[40] Thoudam T, Chanda D, Lee JY, Jung MK, Sinam IS, Kim BG, *et al*. Enhanced Ca(2+)-channeling complex formation at the ER-mitochondria interface underlies the pathogenesis of alcohol-associated liver disease. Nat Commun 2023;14(1):1703. doi:10.1038/s41467-023-37214-4, PMID:36973273.

[41] Patidar P, Hirani N, Bharti S, Baig MS. Key regulators of hepatic stellate cell activation in alcohol liver Disease: A comprehensive review. Int Immunopharmacol 2024;141:112938. doi:10.1016/j.intimp.2024.112938, PMID:39163683.